PHYSICAL REVIEW B **99**, 224504 (2019)

Synthesis and stability of tantalum hydride at high pressures

Jianjun Ying,[1,2,3,*] Xue Li,[4] Eran Greenberg,[5] Vitali B. Prakapenka,[5] Hanyu Liu,[4,†] and Viktor V. Struzhkin[2,‡]
[1]*Department of Physics, and CAS Key Laboratory of Strongly-coupled Quantum Matter Physics, University of Science and Technology of China, Hefei, Anhui 230026, China*
[2]*Geophysical Laboratory, Carnegie Institution of Washington, Washington, DC 20015, USA*
[3]*HPCAT, Geophysical Laboratory, Carnegie Institution of Washington, Argonne, Illinois 60439, USA*
[4]*Innovation Center for Computational Physics Methods and Software & State Key Laboratory of Superhard Materials, College of Physics,130012, Jilin University*
[5]*Center for Advanced Radiation Sources, The University of Chicago, 5640 South Ellis Avenue, Chicago, Illinois 60637, USA*

(Received 5 February 2019; revised manuscript received 12 April 2019; published 11 June 2019)

Although many metal hydrides were predicted by theory, very few of those were so far realized in experiment. Here, we systematically investigated the Ta-H system below 85 GPa, and found that the hexagonal close-packed $TaH_{\sim 2}$ can be gradually transformed into $TaH_{\sim 3}$ above 60 GPa at room temperature. With the help of density-functional theory calculations, the space group of $TaH_{\sim 3}$ can be determined as a $I\bar{4}3d$ phase, which is isostructural to the Domeykite mineral. Such structure is rather rare and was not predicted in the earlier theoretical works due to the large unit cell. We also tried laser heating at high pressures and found that temperature plays a key role in tuning the $TaH_{\sim 3}$ phase to $TaH_{\sim 2}$ phase; however, no other new tantalum hydrides were synthesized. During decompression, the $TaH_{\sim 3}$ was completely decomposed to the $TaH_{\sim 2}$ below 30 GPa. Further experiments are still required for the synthesis of other tantalum polyhydrides at a higher pressure range and for the comparison with the theoretical calculations.

DOI: 10.1103/PhysRevB.99.224504

I. INTRODUCTION

The discovery of superconductivity with superconducting T_c up to 200 K in a compressed H_2S [1,2], in agreement with previous theoretical calculations based on the BCS phonon-mediated theory [3,4], suggested the feasibility of high T_c in compressed hydrogen or hydrogen-rich materials. Recently, superconductivity up to 260 K was observed in LaH_{10} following the theoretical predictions [5–9]. Currently, this discovery motivates scientists to look for high-T_c superconductors in hydrogen-rich materials. Although many hydrides were predicted by theoretical calculations, not many of the predicted phases were confirmed by the experiments until now (for example, LaH_{10} [5], NaH_3 and NaH_7 [10], LiH_2 and LiH_6 [11], FeH_5 [12], $NbH_{2.5}$ and NbH_3 [13], Ni_2H_3 [14], and CoH_2 [15]). It is of significant interest to synthesize other hydrogen-rich materials to confirm or improve the understanding of the theoretically predicted new phases of these fascinating compounds.

Here, we tested the Ta-H system, which has been investigated in detail by the previous theoretical calculations by Zhuang *et al.* [16]. In the previous experiment, various tantalum hydrides were shown to be formed at ambient pressure with the hydrogen content less than 1 [17]. Tantalum dihydride can be formed at relatively low pressures (5 GPa) and can be quenched to ambient pressure at low temperature [18]; however, other tantalum hydrides with higher hydrogen content were not found in previous experiments. Earlier theoretical calculations have predicted several stable hydrogen-rich tantalum hydrides at high pressure, which could be potential high-T_c superconductors with T_c's exceeding 100 K [16], but these predictions still need an experimental confirmation. Here, we performed the high-pressure *in situ* x-ray diffraction measurements of the Ta-H system below 85 GPa. We did not find in our reaction products the tantalum polyhydrides predicted by the previous theoretical calculations. Instead, we did find a cubic phase of $TaH_{\sim 3}$ with a large unit cell which is isostructural with the NbH_3 phase [13,19]. The structure is schematically shown in Fig. 1(c) and is described in more detail in Table S1 in the Supplemental Material [20]. Experiments at higher pressures may be required to synthesize other tantalum polyhydrides predicted by theory. Actually, not much of trihydrides of transition metals were reported, only group IIIB elements (Sc, Y, La) [21–23], Fe [24], Nb [13], and Ir [25] trihydrides are synthesized in the experiment so far. Our work indicates the group VB elements can also form trihydrides with the structure completely different from the other trihydrides.

II. METHODS

A 20-μm-size tantalum foil with a thickness around 4 μm along with small fragments of Au was loaded with hydrogen pressure medium into a diamond-anvil cell with 200-μm culet size. Rhenium was used as gasket material. The x-ray diffraction (XRD) measurements and double-sided laser heating were performed at GeoSoilEnviroCARS

---

[*] yingjj@ustc.edu.cn

[†] hanyuliu@jlu.edu.cn

[‡] vstruzhkin@carnegiescience.edu

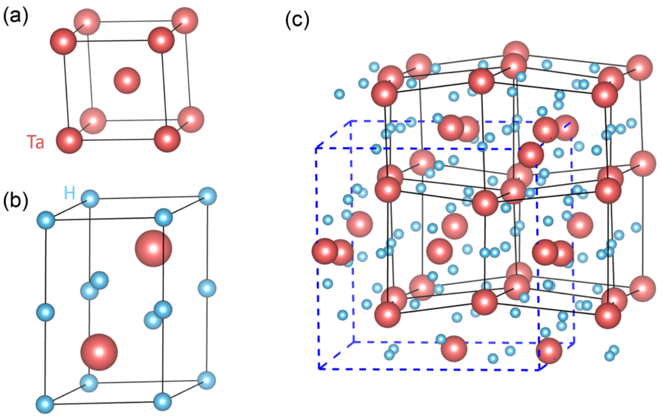

FIG. 1. representation of structures for (a) bcc-Ta, (b) hcp-TaH_2, and (c) cubic TaH_3.

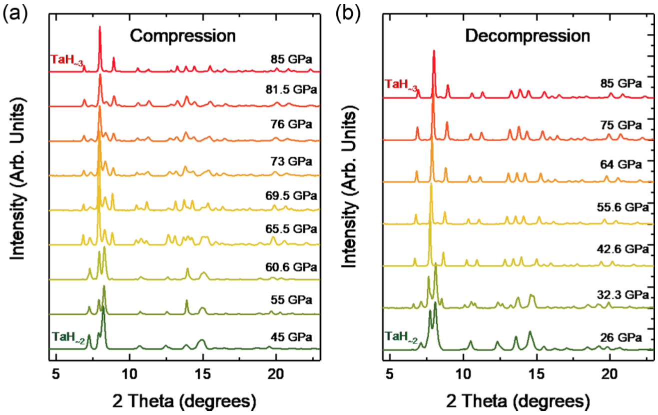

FIG. 2. X-ray diffraction patterns of the Ta-H system under high pressure. (a) During compression, $TaH_{\sim 2}$ phase gradually transforms to the $TaH_{\sim 3}$ phase. (b). The $TaH_{\sim 3}$ phase decomposes to $TaH_{\sim 2}$ phase at low pressure.

(GSECARS) Sector 13 of the Advanced Photon Source at the Argonne National Laboratory. Pressure was determined by the equation of state of gold (Au) [26]. A Pilatus 1M CdTe detector was used to collect angle-dispersive x-ray diffraction with a wavelength of $\lambda = 0.3344$ Å. A sequence of 10 μs × 1000 laser pulses (100-μs delay between pulses) was used to heat the sample to minimize chances of diamond breaking during the heating process. The temperature was determined by using the blackbody radiation. The heating spot was kept away from the gold and Re and was aligned to avoid the sample parts touching the diamond anvil, in order to prevent the contamination by gold and carbon. The two-dimensional images were integrated into intensity versus (2θ) data using the DIOPTAS software [27]. Rietveld refinement was used to refine the data by using the GSAS software [28].

Our structural predictions approach is based on a global minimization of free-energy surfaces merging *ab initio* total-energy calculations through CALYPSO (Crystal structure AnaLYsis by Particle Swarm Optimization) methodology as implemented in CALYPSO code [29,30]. The *ab initio* density-functional theory (DFT) calculations were performed by using DFT as implemented in the Vienna *Ab initio* Simulation Package [31] (VASP) version 5.4. We adopted the all-electron projector-augmented wave potential [32] with Perdew-Burke-Ernzerhof [33] generalized gradient approximation as the exchange-correlation function. Meanwhile, we treated the $1s^1$, $5p^6 5d^3 6s^2$ configurations as valence electrons for H, Ta, respectively. The energy cutoff (600 eV) for the plane-wave expansion of eigenfunctions and proper Monkhorst-Pack meshes with grid spacing of $2\pi \times 0.025$ Å^{-1} were selected to guarantee the enthalpy converges to better than 1 meV/atom. The dynamically stability was checked by density-functional perturbation theory as implemented in the PHONOPY code [34]. The crystal structures were drawn by the VESTA package [35].

III. RESULTS AND DISCUSSION

Upon compression, Ta already reacted with hydrogen to form hexagonal close-packed (hcp)-$TaH_{\sim 2}$ at our first pressure point (45 GPa), consistent with the previous result [18]. The structures of bcc-Ta and hcp-TaH_2 are shown in Figs. 1(a) and 1(b). Peaks emerge after increasing the pressure above 60 GPa at ambient temperature as shown in Fig. 2(a), indicating that a tantalum hydride phase has formed. The time interval for each pressure change was about 10 min in our experiment. By using the XRD refinement and theoretical calculations, we determined this tantalum hydride to be $TaH_{\sim 3}$, as discussed in detail below. The structure of cubic TaH_3 can be visualized as a distorted bcc structure shown in Fig. 1(c). Such structure is rather rare; it was observed only in Domeykite mineral Cu_3As and in compressed NbH_3 phase according to our knowledge [13,19]. After further increasing the pressure, the $TaH_{\sim 3}$ phase reflections intensity becomes stronger, while the $TaH_{\sim 2}$ phase reflections becomes weaker. Above 85 GPa, nearly all $TaH_{\sim 2}$ phase transforms to the $TaH_{\sim 3}$ phase. Upon decompression, the $TaH_{\sim 3}$ phase remains stable above 42 GPa as shown in Fig. 2(b). The $TaH_{\sim 3}$ phase is gradually decomposing to $TaH_{\sim 2}$ phase at pressures below 40 GPa. Below 26 GPa, no $TaH_{\sim 3}$ phase can be detected

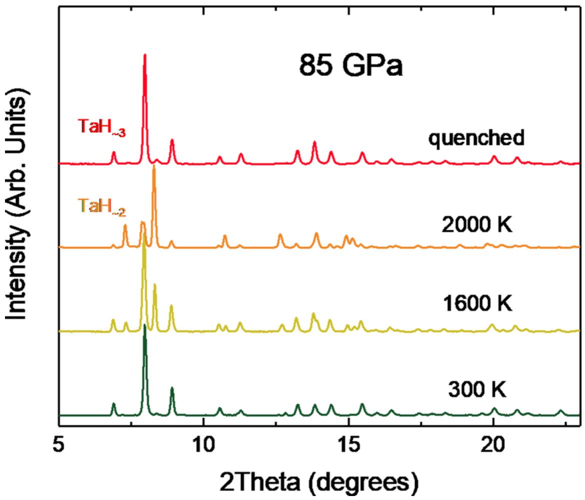

FIG. 3. X-ray diffraction spectrum of Ta-H system at high temperature with the pressure of 85 GPa. The $TaH_{\sim 3}$ phase decomposes to $TaH_{\sim 2}$ phase at high temperature.

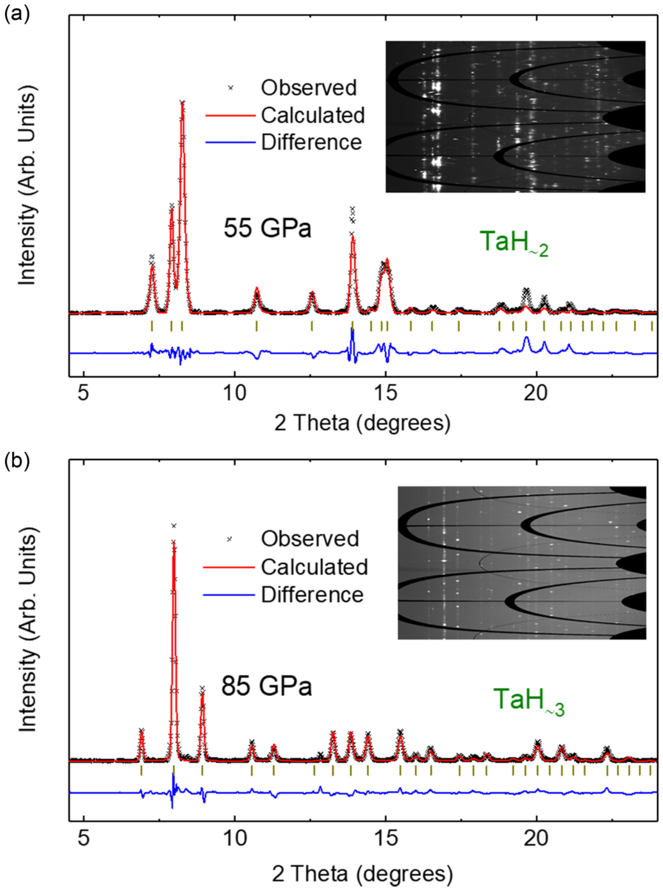

FIG. 4. XRD pattern and Rietveld refinement for $\mathrm{TaH}_{\sim 2}$ phase (a) and $\mathrm{TaH}_{\sim 3}$ phase (b) with wavelength $\lambda = 0.3344$ Å. The insets show the cake-type image of the two dimensional x-ray-diffraction patterns.

by x-ray-diffraction measurements. The roughly estimated degree of conversion for $\mathrm{TaH}_{\sim 3}$ is shown in Fig. S1 in the Supplemental Material [20]. In order to synthesize other tantalum hydrides, we performed diffraction experiments upon laser heating at high pressures. Unfortunately, we found that $\mathrm{TaH}_{\sim 3}$ phase decomposes to $\mathrm{TaH}_{\sim 2}$ at high temperatures rather than forming other tantalum polyhydrides as shown in Fig. 3. The $\mathrm{TaH}_{\sim 2}$ phase becomes more abundant as the temperature increases, and it becomes the major phase once the temperature reaches 2000 K. However, the major phase of the sample quenched to room temperature reverts back to the $\mathrm{TaH}_{\sim 3}$. These results indicate that the $\mathrm{TaH}_{\sim 3}$ phase is stable at high pressure and low temperature. Unlike in the other known metal hydrides, the laser heating method appears to be not an ideal tool to synthesize the predicted tantalum polyhydrides, within the studied pressure range.

In order to identify the structure of $\mathrm{TaH}_{\sim 3}$, we have also performed the Rietveld refinement for both $\mathrm{TaH}_{\sim 2}$ and $\mathrm{TaH}_{\sim 3}$ as shown in Fig. 4. The powder-diffraction data for $\mathrm{TaH}_{\sim 2}$ can be refined by using the space group $P6_3mc$ indicated by the theoretical calculation [16], and the structure of the $\mathrm{TaH}_{\sim 3}$ phase can be refined by using the space group $I\bar{4}3d$. The lattice parameter is 6.796(1) Å and the refined Ta atomic coordinates are [0.5327(2), 0.0327(2), 0.4673(2)]. These results indicate the validity of the suggested $\mathrm{TaH}_{\sim 2}$ and $\mathrm{TaH}_{\sim 3}$ structures.

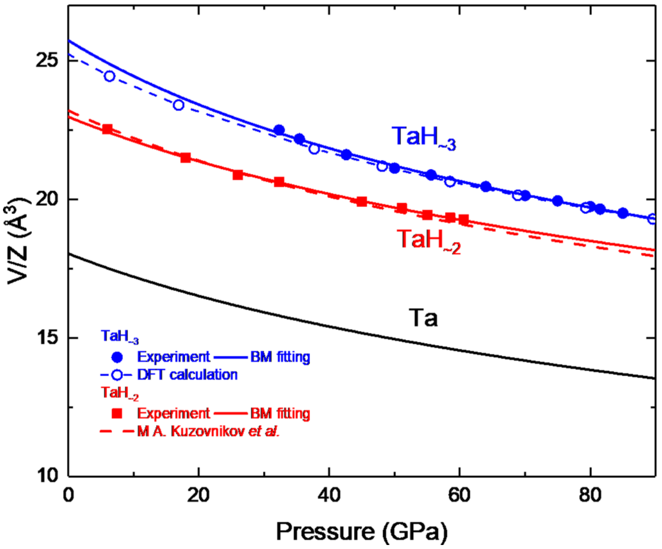

FIG. 5. Volume per Ta atom (*V/Z*) as a function of pressure for Ta, $\mathrm{TaH}_{\sim 2}$, and $\mathrm{TaH}_{\sim 3}$. The solid lines represent the BM fit results as given in Table I. The experimental results for $\mathrm{TaH}_{\sim 3}$ match well the DFT calculation results. The dashed red line is the equation of state for $\mathrm{TaH}_{\sim 2}$ which is determined below 41 GPa in previous work [18].

We can plot the volume per Ta atom (*V/Z*) as a function of pressure for Ta, $\mathrm{TaH}_{\sim 2}$, and $\mathrm{TaH}_{\sim 3}$ as shown in Fig. 5. The blue and red solid lines are Birch-Murnaghan (BM) fitting results for $\mathrm{TaH}_{\sim 3}$ and $\mathrm{TaH}_{\sim 2}$, respectively. The detailed fitting parameters are listed in Table I. Our measured lattice parameter for $\mathrm{TaH}_{\sim 2}$ is consistent with previous results, which were obtained at pressures less than 41 GPa [18]. We also compare the measured lattice parameters with the theoretical calculations at high pressure for $\mathrm{TaH}_{\sim 3}$. The measured lattice parameters match well the theoretically predicted ones.

In recent studies, it was shown that the approach was successful in the prediction of the high-temperature superconductivity, for example in LaH_{10} [5,6] and other polyhydrides. Herein, we studied the stability for different predicted structures using the convex-hull diagram and considering the zero-point energy (ZPE). We performed the predictions by employing simulation cells up to 8 formula units (f.u.) at 100 GPa. The calculated convex-hull of Ta-H system is shown in Fig. 6. It is noteworthy that we found the lower-energy and

TABLE I. Volume per formula unit at ambient pressure *V*/(Ta atom), the bulk modulus B_0, the pressure derivative of the bulk modulus B_0', as derived from fitting results by using the BM equation of state. Numbers between parentheses represent fitting or published errors bars.

	Crystal structure	V_0/Z(Å^3)	B_0 (GPa)	B_0'	Reference
Ta	bcc	18.04	195(5)	3.4(0.1)	[36]
$\mathrm{TaH}_{\sim 2}$	hcp	22.97(0.15)	239(20)	4(fixed)	This work
		23.2(0.2)	210(20)	4(fixed)	[18]
$\mathrm{TaH}_{\sim 3}$	$I\bar{4}3d$(220)	25.73(0.2)	176(15)	4(fixed)	This work

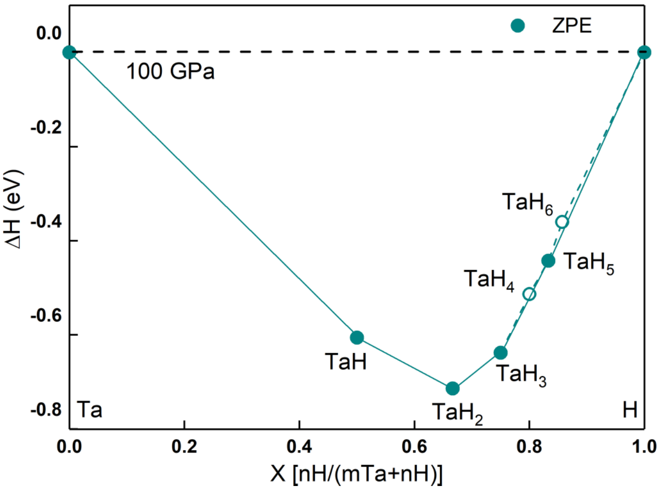

FIG. 6. Calculated convex-hull of Ta-H system at 100 GPa considering the ZPE.

higher-symmetry cubic phase of TaH_3 in comparison to the previous work [16], with the energy difference of about 27 meV/atom. We also list the predicted structures of TaH_2, TaH_4, and TaH_5 in the Supplemental Material [20]. Since we used ZPE and larger simulation unit cell in our calculations, the predicted structures of TaH_x are different from the ones obtained in the previous work [16]. In order to explore the physical properties of TaH_3, we calculated the electronic states of the stable structure for TaH_3 at 100 GPa as shown in Fig. 7. The band structure shows that TaH_3 is a metallic phase at high pressures. The absence of any imaginary frequency modes in the whole Brillouin zone suggests the dynamical stability of TaH_3 at high pressures as shown in Fig. 7(b). The application of the Allen-Dynes modified McMillan's equation reveals a favorable superconducting critical temperature, which reaches 15 K at 100 GPa and increases with decreasing pressure ($T_c = 23$ K at 80 GPa), which needs further experimental confirmation. Although the predicted T_c in TaH_3 is relatively low compared to the other metal polyhydrides, relatively low pressure and no additional heating are needed to synthesize the pure phase of $TaH_{\sim 3}$, which makes it relatively easy to perform the future transport and/or magnetic experiments to detect the superconductivity in this material.

Although earlier theoretical calculations have predicted various hydrogen-rich tantalum hydrides, however, in our experiment, we do not observe the TaH_n (n larger than 2) phases predicted earlier. Instead, we observed another cubic phase of $TaH_{\sim 3}$. The structure of $TaH_{\sim 3}$ is isostructural to the Domeykite mineral Cu_3As; such structure contains 16 f.u., which is very rare. This peculiar structure can also be seen as a distorted *Pm*-3*n* (Nb_3Sn-type) structure. Ta-H system shows some similarities with the Nb-H system, which was reported previously [13]. The $TaH_{\sim 3}$ phase is stable above 30 GPa at ambient temperature in our experiment. We also performed calculation of the transition pressure from TaH_2 to TaH_3 at $T = 0$ K as shown in the Supplemental Material [20]. We found that TaH_2 will transform to TaH_3 phase at around 24 GPa, which is consistent with our experimental results. NbH_2 with hcp structure and distorted bcc phase of NbH_3 were observed before; however, there are many other competing high-pressure phases in Nb-H system, such as double hcp-$NbH_{2.5}$, and fcc-$NbH_{2.5-3}$; and the Nb hydrides are usually not observed in a single phase setting. In Ta-H system, the phase diagram is simple; only the hcp $TaH_{\sim 2}$ and the $I\bar{4}3d$ structure of $TaH_{\sim 3}$ are observed at high pressure. Consequently, the pure phase of $TaH_{\sim 3}$ can be obtained, which is crucial for future physical property measurements.

We would like to comment here on the stoichiometry of the synthesized samples. It is notoriously difficult to exactly determine the hydrogen content in the high-pressure hydride phases. It is a common practice that the volume expansion is used to estimate the hydrogen content in the hydride. At 60 GPa, $V(TaH_{\sim 2}) - V(Ta) = 4.68\ \text{Å}^3$, and since the hydrogen content H/Ta in hcp $TaH_{\sim 2}$ was measured to be 2.2

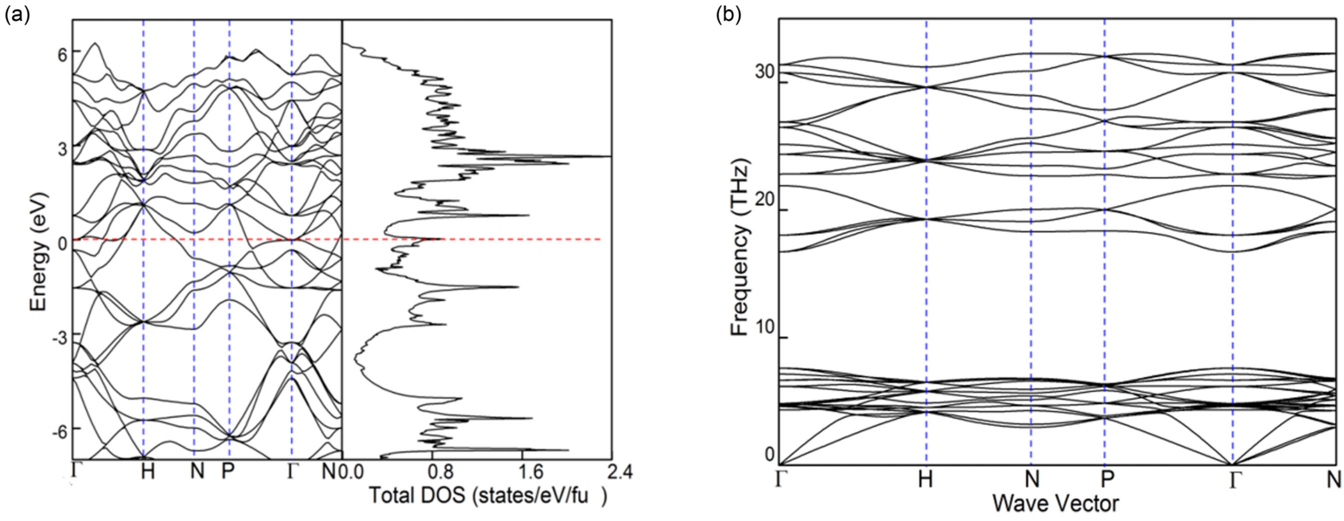

FIG. 7. (a) Calculated band structure and density of states for the predicted cubic TaH_3 phase at 100 GPa. (b) Calculated phonon dispersion for TaH_3 at 100 GPa. The absence of any imaginary frequency modes in the whole Brillouin zone suggests the dynamical stability of TaH_3 at high pressures.

by thermodesorption [18], the extra volume ΔV_H added by each hydrogen atom is about $2.13\,\text{Å}^3$. For the $TaH_{\sim 3}$, the volume expansion $V(TaH_{\sim 3}) - V(Ta) = 6.07\,\text{Å}^3$. Thus, we can roughly estimate the H/Ta in $TaH_{\sim 3}$ to be about 2.85, which is quite close to 3. For this reason, we believe that the synthesized TaH_3 phase could be close to the stoichiometric composition, given the uncertainties involved in such estimation procedure. The Ta atom positions and lattice parameters obtained from the refinement of the $TaH_{\sim 3}$ are almost identical to the ones obtained from the calculations, which strongly supports nearly stoichiometric composition in the synthesized $TaH_{\sim 3}$.

IV. CONCLUSION

In conclusion, we attempted to synthesize predicted tantalum polyhydrides at high pressure. We do not observe the previously theoretically predicted tantalum polyhydride phases. Instead, we synthesized a cubic phase of $TaH_{\sim 3}$ with a large unit cell. Unlike the other metal hydrides, laser heating did not help to synthesize polyhydrides in the Ta-H system. The $TaH_{\sim 3}$ phase decomposes to the $TaH_{\sim 2}$ phase under heating. Tantalum polyhydrides with higher hydrogen content may exist at higher pressures, and further experiments are needed to clarify if the other theoretically predicted tantalum polyhydrides could be stabilized at high pressures above 85 GPa.

ACKNOWLEDGMENTS

High-pressure experiments were supported by Department of Energy (DOE)/BES under Contract No. DE-FG02-99ER45775. V.V.S. acknowledges support from the Thousand Talent Program by the State Council of the People's Republic of China. Portions of this work was performed at GSECARS (The University of Chicago, Sector 13), Advanced Photon Source, Argonne National Laboratory. GeoSoilEnviroCARS is supported by the National Science Foundation - Earth Sciences (Grant No. EAR - 1634415) and Department of Energy- GeoSciences (Grant No. DE-FG02-94ER14466). This research used resources of the APS, a US DOE Office of Science User Facility operated for the DOE Office of Science by Argonne National Laboratory under Contract No. DE-AC02-06CH11357.

---

[1] A. P. Drozdov, M. I. Eremets, I. A. Troyan, V. Ksenofontov, and S. I. Shylin, Nature (London) **525**, 73 (2015).

[2] I. Troyan, A. Gavriliuk, R. Rüffer, A. Chumakov, A. Mironovich, I. Lyubutin, D. Perekalin, A. P. Drozdov, and M. I. Eremets, Science **351**, 1303 (2016).

[3] D. Duan *et al.*, Sci. Rep. **4**, 6968 (2014).

[4] Y. Li, J. Hao, H. Liu, Y. Li, and Y. Ma, J. Chem. Phys. **140**, 174712 (2014).

[5] Z. M. Geballe, H. Liu, A. K. Mishra, M. Ahart, M. Somayazulu, Y. Meng, M. Baldini, and R. J. Hemley, Angew. Chem. Int. Ed. **57**, 688 (2018).

[6] H. Liu, I. I. Naumov, R. Hoffmann, N. W. Ashcroft, and R. J. Hemley, Proc. Natl. Acad. Sci. USA **114**, 6990 (2017).

[7] M. Somayazulu, M. Ahart, A. K. Mishra, Z. M. Geballe, M. Baldini, Y. Meng, V. V. Struzhkin, and R. J. Hemley, Phys. Rev. Lett. **122**, 027001 (2019).

[8] A. P. Drozdov *et al.*, Nature (London) **569**, 528 (2019).

[9] L. Zhang, Y. Wang, J. Lv, and Y. Ma, Nat. Rev. Mater. **2**, 17005 (2017).

[10] V. V. Struzhkin, D. Y. Kim, E. Stavrou, T. Muramatsu, H.-k. Mao, C. J. Pickard, R. J. Needs, V. B. Prakapenka, and A. F. Goncharov, Nat. Commun. **7**, 12267 (2016).

[11] C. Pépin, P. Loubeyre, F. Occelli, and P. Dumas, Proc. Natl. Acad. Sci. USA **112**, 7673 (2015).

[12] C. M. Pépin, G. Geneste, A. Dewaele, M. Mezouar, and P. Loubeyre, Science **357**, 382 (2017).

[13] G. Liu, S. Besedin, A. Irodova, H. Liu, G. Gao, M. Eremets, X. Wang, and Y. Ma, Phy. Rev. B **95**, 104110 (2017).

[14] J. Ying, H. Liu, E. Greenberg, V. B. Prakapenka, and V. V. Struzhkin, Phy. Rev. Mater. **2**, 085409 (2018).

[15] M. Wang, J. Binns, M.-E. Donnelly, M. Peña-Alvarez, P. Dalladay-Simpson, and R. T. Howie, J. Chem. Phys. **148**, 144310 (2018).

[16] Q. Zhuang, X. Jin, T. Cui, Y. Ma, Q. Lv, Y. Li, H. Zhang, X. Meng, and K. Bao, Inorg. Chem. **56**, 3901 (2017).

[17] A. W. Szafrański, M. Tkacz, S. Majchrzak, and H. Züchner, J. Less-Common Met. **101**, 523 (1984).

[18] M. A. Kuzovnikov, M. Tkacz, H. Meng, D. I. Kapustin, and V. I. Kulakov, Phy. Rev. B **96**, 134120 (2017).

[19] G. Gao, R. Hoffmann, N. W. Ashcroft, H. Liu, A. Bergara, and Y. Ma, Phy. Rev. B **88**, 184104 (2013).

[20] See Supplemental Material at http://link.aps.org/supplemental/10.1103/PhysRevB.99.224504 for details of the $TaH_{\sim 3}$ conversion ratio, calculated transition pressure and structural parameters for tantalum hydrides.

[21] V. E. Antonov, I. O. Bashkin, V. K. Fedotov, S. S. Khasanov, T. Hansen, A. S. Ivanov, A. I. Kolesnikov, and I. Natkaniec, Phy. Rev. B **73**, 054107 (2006).

[22] W. L. Korst and J. C. Warf, Inorg. Chem. **5**, 1719 (1966).

[23] M. Mansmann and W. E. Wallace, J. Phys. France **25**, 454 (1964).

[24] C. M. Pépin, A. Dewaele, G. Geneste, P. Loubeyre, and M. Mezouar, Phys. Rev. Lett. **113**, 265504 (2014).

[25] T. Scheler, M. Marqués, Z. Konôpková, C. L. Guillaume, R. T. Howie, and E. Gregoryanz, Phys. Rev. Lett. **111**, 215503 (2013).

[26] Y. Fei, A. Ricolleau, M. Frank, K. Mibe, G. Shen, and V. Prakapenka, Proc. Natl. Acad. Sci. USA **104**, 9182 (2007).

[27] C. Prescher and V. B. Prakapenka, High Pressure Res. **35**, 223 (2015).

[28] A. C. Larson and R. B. Von Dreele, Los Alamos National Laboratory Report No. LAUR 86-748, 1994.

[29] Y. Wang, J. Lv, L. Zhu, and Y. Ma, Phy. Rev. B **82**, 094116 (2010).

[30] Y. Wang, J. Lv, L. Zhu, and Y. Ma, Comput. Phys. Commun. **183**, 2063 (2012).

[31] G. Kresse and J. Furthmüller, Phy. Rev. B **54**, 11169 (1996).

[32] P. E. Blöchl, Phy. Rev. B **50**, 17953 (1994).

[33] J. P. Perdew, K. Burke, and M. Ernzerhof, Phys. Rev. Lett. **77**, 3865 (1996).

[34] A. Togo, F. Oba, and I. Tanaka, Phy. Rev. B **78**, 134106 (2008).

[35] K. Momma and F. Izumi, J. Appl. Crystallogr. **41**, 653 (2008).

[36] H. Cynn and C.-S. Yoo, Phy. Rev. B **59**, 8526 (1999).